THE FORMATION OF MACROTWINS IN NiAl MARTENSITE

J.M. BALL* (ball@maths.ox.ac.uk)
Mathematical Institute, University of Oxford, 24-29 St. Giles', Oxford OX1 3LB, U.K.

D. SCHRYVERS† (schryver@ruca.ua.ac.be)
EMAT, University of Antwerp, RUCA, Groenenborgerlaan 171, B-2020 Antwerpen, Belgium

1. Introduction.

Using high resolution electron microscopy, Boullay & Schryvers [6] observed and documented interesting macrotwin interfaces in bulk and splat-cooled $Ni_{65}Al_{35}$ polycrystals. This alloy undergoes a cubic (bcc) to tetragonal (bct) martensitic transformation. The macrotwin interfaces separate two different plates of martensite, each plate involving the same two martensitic variants but with microtwin interfaces that are nearly orthogonal. They measured the orientations both of the microtwin interfaces and of the rotations of the variants comprising the microtwins, in the vicinity of the macrotwin plane and at distances of up to several hundred nanometres from this plane. In addition, they described atomic scale details of the macrotwin region, in particular identifying two different ways in which the microtwins meet at the macrotwin plane, one in which they appear to cross, and the other in which they meet in a stepped configuration (see Fig. 1). In the bulk samples, which form the main focus of this paper, the grain-size is large (of the order of 1mm) compared to that of the macrotwins. In the splat-cooled samples it is smaller (of the order of 1μm).

It is natural to believe that these macrotwins arise from coalescence of two different martensitic plates nucleated in the austenite at different points, each having a different habit plane separating the martensite from the austenite, that propagate towards each other, eliminating the austenite

* Research supported by EC TMR Contract FMRX-CT98-0229 on 'Phase Transitions in Crystalline Solids'.

† Research supported by the above EC contract and the IUAP project of the Belgium Federal government on "Reduced Dimensionality Systems" (P4/10).

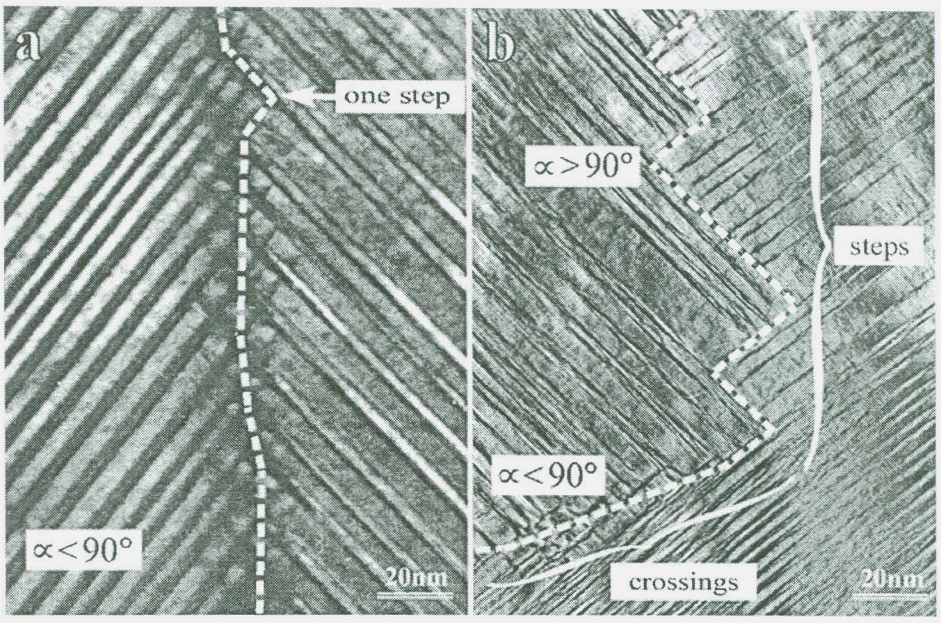

Figure 1. Low magnification images of macrotwin boundaries of (a) crossing, and (b) step type. The angles α indicated are those between the microtwin interfaces in each plate.

between them. However for the bulk and splat-cooled samples used in the experiments the transformation is too fast to observe the sequence of events leading to the final martensitic microstructure, and so indirect evidence is needed to confirm the above scenario.

Some such evidence is provided by correlating details of the observed microstructures with predictions of the nonlinear elasticity model of martensitic transformations (see Ball & James [2], [3]), a model that incorporates the crystallographic theory of martensite (Wechsler, Lieberman & Read [13]) into a much more general framework. (For corresponding linearized models see [8], [9], [10], [11], [12], [5].) We treat the sample as if it were a single crystal, ignoring constraints imposed by neighbouring grains. In terms of the kind of calculations made, this is justified provided the microstructures have close to zero energy (the zero of energy being taken to be that of a pure variant of martensite or of undistorted austenite, these energies being equal at the transformation temperature θ_c).

A calculation of Bhattacharya [4] related to the so-called *wedge microstructure* shows that it is impossible for two different martensitic plates, involving the same two martensitic variants and having different habit plane normals, to be compatible at zero energy at θ_c across any macrotwin plane. This means that if the observed macrotwins arise by coalescence of two

such plates, then stresses must be accommodated in the vicinity of the macrotwin boundaries. Nevertheless one can calculate (see Section 3) the relative orientations of the microtwin planes and of the different variants in the two plates prior to meeting of the habit planes, as well as the relative volume fractions of the two variants in each plate. These volume fractions are predicted by the theory to be either the same in each plate, or reversed. In all the examples of macrotwins observed by Boullay & Schryvers the volume fractions in the two plates were found to be almost the same and to be close to that predicted by the theory for a single plate in contact with the austenite, suggesting that these volume fractions remain more or less unchanged as the plates coalesce.

On the other hand one can do a second calculation (see Section 4) to determine whether two plates involving the same two martensitic variants and having the same volume fractions can be compatible at zero energy across a macrotwin interface, without requiring, as in the Bhattacharya calculation, that these plates are also compatible with the austenite. This calculation shows that the macrotwin normal must be a prior [100] cubic plane, and delivers relative orientations of the microtwin planes and variants that are different from those of the first calculation.

It turns out that both these calculations seem to be relevant. The first predicts with satisfactory accuracy many details of the experimental data at a sufficiently large distance (more than 500nm) from the macrotwin interface, while for the case of the crossing-type macrotwins, the second correctly predicts the trends in the relative orientations that are observed in an intermediate region between 50 and 500nm from the macrotwin interface. In this intermediate region the microtwin interfaces curve, this curvature being accompanied by a corresponding rotation of the crystal lattice. In the region very close to the macrotwin interface, from 0 to 50nm from it, there is still an apparent macroscopic curvature of the microtwin interfaces, but at the atomic level this is seen to be achieved without lattice rotation, the microtwin interfaces consisting of planar sections having the same orientation and separated by nearly equidistant atomic scale ledges. Presumably lattice curvature is the energetically optimal way to relieve small stresses, while ledges, for which the energy is concentrated in dislocations, are best for relieving the larger stresses close to the macrotwin interface. The situation for the stepped-type macrotwins closer to the macrotwin interface is somewhat different, and is described in more detail in [7].

In this paper we give precise statements and a few details of these calculations, the results of which are used for the experimental comparisons in [6], and which led to some of the observations made there. A more comprehensive treatment will appear elsewhere.

2. The nonlinear elasticity model of martensitic transformations

This model is based on an elastic free-energy density $\varphi(F,\theta)$, in terms of which the total free-energy of a single crystal at temperature θ is given by

$$I_\theta(y) = \int_\Omega \varphi(\nabla y(x),\theta)\,dx. \tag{2.1}$$

In (2.1) $y(x) = (y_1(x), y_2(x), y_3(x))$ denotes the deformed position of the material point of the crystal occupying the point $x = (x_1, x_2, x_3)$ in the region Ω occupied by the crystal in a reference configuration, which we take to be undistorted austenite at the transformation temperature θ_c, and $\nabla y(x)$ denotes the deformation gradient, namely the 3×3 matrix $(\partial y_i/\partial x_j)$. The free-energy density is assumed to be frame-indifferent, that is

$$\varphi(RF,\theta) = \varphi(F,\theta) \tag{2.2}$$

for all F in the set $M^{3\times 3}_+$ of 3×3 matrices with positive determinant, and all R in the set $SO(3)$ of rotations. Further, φ is assumed to satisfy the material symmetry condition

$$\varphi(FQ,\theta) = \varphi(F,\theta) \tag{2.3}$$

for all rotations Q in the point group $\mathcal{S}$ of the crystal, in our case given by $\mathcal{S} = \mathcal{P}^{24}$, the set of rotations of a cube into itself. By adding a suitable function of θ to φ we may assume that $\min\varphi(\cdot,\theta) = 0$, so that the set $K(\theta)$ of energy-minimizing deformation gradients is given by

$$K(\theta) = \{F \in M^{3\times 3}_+ : \varphi(F,\theta) = 0\}$$

By (2.2), (2.3) we have that

$$K(\theta) = RK(\theta)Q \qquad \text{for all } R \in SO(3), Q \in \mathcal{S}.$$

More specifically, for a cubic-to-tetragonal transformation, $K(\theta_c)$ is assumed to have the form

$$K(\theta_c) = SO(3) \cup \bigcup_{i=1}^{3} SO(3)U_i,$$

where $U_1 = \text{diag}\,(\eta_3,\eta_1,\eta_1)$, $U_2 = \text{diag}\,(\eta_1,\eta_3,\eta_1)$, and $U_3 = \text{diag}\,(\eta_1,\eta_1,\eta_3)$ are the transformation strains of the three martensitic variants, and where $\eta_1 > 0, \eta_3 > 0$ are the deformation parameters.

We can identify zero-energy microstructures with sequences of deformations $y^{(j)}$ such that $I_{\theta_c}(y^{(j)}) \to 0$ as $j \to \infty$, or with the *Young measures* $(\nu_x)_{x\in\Omega}$ corresponding to the deformation gradients $Dy^{(j)}$ of such

sequences. For each $x \in \Omega$, ν_x is a probability measure on $M^{3\times 3}_+$ describing the limiting probability of finding particular values of $Dy^{(j)}(z)$ for very large j when z is sampled at random from a small ball $B(x,r)$ of radius r about the point x (see [1]). More precisely, for a subset E of $M^{3\times 3}_+$

$$\nu_x(E) = \lim_{r\to 0}\lim_{j\to\infty} \frac{\text{volume } \{z \in B(x,r) : Dy^{(j)}(z) \in E\}}{\text{volume } B(x,r)}.$$

Since $I_{\theta_c}(y^{(j)}) \to 0$, we have that ν_x is supported in $K(\theta_c)$ for each x; that is, the limiting probability of finding a value for the deformation gradient outside $K(\theta_c)$ is zero.

As is well known, twins correspond to rank-one connections

$$A - B = a \otimes n \tag{2.4}$$

between two of the martensitic energy wells $SO(3)U_i$, A and B being the deformation gradients on opposite sides of the twin plane, which has normal n. Taking without loss of generality twins involving the first two variants and $B = U_1$, the two possible twins with $A \in SO(3)U_2$ are given by

$$a = \sqrt{2}\frac{\eta_3^2 - \eta_1^2}{\eta_1^2 + \eta_3^2}(-\eta_3, \kappa\eta_1, 0),\ n = \frac{1}{\sqrt{2}}(1, \kappa, 0), \tag{2.5}$$

where $\kappa = \pm 1$. The angle of rotation γ between variants across a microtwin plane is given by

$$\gamma = \cos^{-1}\frac{2\eta_1\eta_3}{\eta_1^2 + \eta_3^2}. \tag{2.6}$$

A martensitic plate with twins A, B in the volume fraction λ to $1-\lambda$ corresponds to the Young measure

$$\nu_x = \lambda\delta_A + (1-\lambda)\delta_B,$$

where δ_G denotes the Dirac mass at G defined by $\delta_G(E) = 1$ if $G \in E$, $\delta_G(E) = 0$ otherwise. The corresponding macroscopic deformation gradient is $F = \lambda A + (1-\lambda)B$.

In order for such a plate to be compatible with undistorted austenite across the habit plane $\{x \cdot m = k\}$ the equation

$$\lambda A + (1-\lambda)B = \mathbf{1} + b \otimes m \tag{2.7}$$

must hold for some vector b, this being necessary and sufficient for there to exist a sequence $y^{(j)}$ with gradient $Dy^{(j)}$ having Young measure ν_x given by

$$\nu_x = \begin{cases} \delta_{\mathbf{1}} & \text{if } x \cdot m < k, \\ \lambda\delta_A + (1-\lambda)\delta_B & \text{if } x \cdot m > k. \end{cases}$$

The solutions $A \in SO(3)U_i$, $B \in SO(3)U_j$, $\lambda \in [0,1]$, b, m of (2.4), (2.7) are given by the formulae of the crystallographic theory of martensite [13]. Taking $i = 1, j = 2$ we have that $A = QU_1$, $B = Q(U_1 + a \otimes n)$ with $Q \in SO(3)$ and a, n given by (2.5), that $\lambda = \lambda^*$ or $1 - \lambda^*$, where

$$\lambda^* = \frac{1}{2}\left(1 - \sqrt{\frac{2(\eta_3^2 - 1)(\eta_1^2 - 1)(\eta_1^2 + \eta_3^2)}{(\eta_3^2 - \eta_1^2)^2} + 1}\right),$$

and that

$$m = (\frac{1}{2}\chi(\delta + \tau), \frac{1}{2}\chi\kappa(\tau - \delta), 1), \tag{2.8}$$

$$b = (\frac{1}{2}\chi\zeta(\delta + \tau), \frac{1}{2}\chi\zeta\kappa(\tau - \delta), \beta), \tag{2.9}$$

for $\lambda = \lambda^*$, with the sign before τ changed if $\lambda = 1 - \lambda^*$. Here

$$\delta = [(\eta_3^2 + \eta_1^2 - 2)(1 - \eta_1^2)^{-1}]^{\frac{1}{2}}, \tag{2.10}$$

$$\tau = [(2\eta_1^2\eta_3^2 - \eta_1^2 - \eta_3^2)(1 - \eta_1^2)^{-1}]^{\frac{1}{2}}, \tag{2.11}$$

$$\zeta = \frac{1 - \eta_1^2}{1 + \eta_3}, \ \beta = \frac{\eta_3(\eta_1^2 - 1)}{1 + \eta_3}, \ \chi = \pm 1. \tag{2.12}$$

These solutions exist provided the inequalities

$$\eta_1^2 + \eta_3^2 < 2 \text{ if } \eta_1 > 1; \quad \eta_1^{-2} + \eta_3^{-2} < 2 \text{ if } \eta_1 < 1 \tag{2.13}$$

hold. For details see [2].

3. Calculations for macrotwins (i)

Two different martensitic plates with macroscopic deformation gradients $\mathbf{1} + b \otimes m, \mathbf{1} + \bar{b} \otimes \bar{m}$ can only be compatible if $b \otimes m - \bar{b} \otimes \bar{m}$ has rank one, that is if b is parallel to $\bar{b}$ or m is parallel to $\bar{m}$. Using the formulae (2.8)-(2.12), Bhattacharya [4] showed that this cannot happen if the two plates comprise the same two variants, and that it can happen for plates which together use all three variants if and only if

$$\eta_1^2 = \frac{(1 - \eta_3^2)^2 + 4\eta_3^2(1 + \eta_3^2)}{(1 - \eta_3^2)^2 + 8\eta_3^4}, \tag{3.1}$$

in which case the macrotwin plane is $[110]_{B2}$ and the microtwin interfaces meet at an angle of about 120°. This case is observed in $Ni_{65}Al_{35}$, for which

(3.1) is nearly satisfied, but we do not consider it further in this paper. Instead we concentrate on the case of macrotwins involving only two variants, whose microtwin interfaces meet at about 90°, for which the calculation in [4] shows that compatibility cannot be achieved at zero energy, and thus that the deformation close to the macrotwin interface cannot be stress-free.

We take the viewing direction in the TEM images to be $e_3 = [001]_{B2}$. Since there is no austenite present it is not possible to check the accuracy of this assumption directly. The situation is also complicated by various imaging issues that are discussed more fully in [6]. Fortunately the results of the calculations are insensitive to changes in the viewing direction of a few degrees. To fix orientation we take the e_3 axis to be pointing into the sample plane, with the $e_2 = [010]_{B2}$ axis horizontal and the $e_1 = [100]_{B2}$ axis vertical. From (2.8) we see that e_3 is not parallel to the habit plane. As a consequence, the microtwin plane with undeformed normal $n = \frac{1}{\sqrt{2}}(1, \kappa, 0)$ is not parallel to the viewing direction, but has normal n' parallel to $(\mathbf{1} + b \otimes m)^{-T} n$, from which it follows that n' is obtained by rotating n about $n \wedge n'$ clockwise through the angle

$$\theta = \cos^{-1} \frac{1 + \eta_3 z^2}{(1 + \eta_3) z}, \qquad z = \sqrt{\frac{\eta_1^{-2} + \eta_3^{-2}}{2}}.$$

The angle of rotation of the trace of the microtwin plane in $\{x_3 = 0\}$ is different and is given by

$$\psi = \cos^{-1} \frac{\eta_1^2 \eta_3 - \frac{1}{2}\zeta\tau^2}{\sqrt{\eta_1^4 \eta_3^2 - \zeta\tau^2 \eta_1^2 \eta_3 + \frac{1}{4}\zeta^2\tau^2(\delta^2 + \tau^2)}}, \tag{3.2}$$

the sense of rotation being clockwise in the case $\lambda = \lambda^*$ (corresponding to vol $U_1 >$ vol U_2) if $\kappa = 1$ and anticlockwise if $\kappa = -1$ (with the orientation described above).

The deformation parameters are measured from the HRTEM images assuming that the transformation strain is volume-preserving, giving values $\eta_1 = .93, \eta_3 = 1.15$ used below. These values satisfy (2.13). In particular, from (3.2) we get $\psi = 1.88°$.

Suppose that a macrotwin is formed by coalescence of two martensitic plates, Plate I and Plate II, comprising the variants U_1 and U_2 in the same relative volume fractions λ^* but using different microtwins, namely with normals $n = \frac{1}{\sqrt{2}}(1, 1, 0)$ for Plate I, and $n = \frac{1}{\sqrt{2}}(1, -1, 0)$ for Plate II. We suppose that the macrotwin normal N is either e_1 or e_2. That these are preferred normals is motivated in Section 4.

The above calculations imply that for $N = e_1$ the microtwin traces in the two plates make an angle $\alpha = 90° + 2\psi = 93.76° > 90°$ with one another, while for $N = e_2$ we have $\alpha = 90° - 2\psi = 86.24° < 90°$.

The rotations of the variants in each plate can also be calculated. Consider, for example, the U_1 variant in a macrotwin with $\kappa = 1$, $\lambda = \lambda^*$. In the austenite a $[010]_{B2}$ plane intersects $\{x_3 = 0\}$ in a line $x_2 =$ constant, while in the U_1 variant of the macrotwin the corresponding line of intersection for a prior $[010]_{B2}$ plane is rotated anticlockwise through an angle of 4.23°. In the U_2 variant the lines of intersection of prior $[100]_{B2}$ planes with $\{x_3 = 0\}$ are rotated clockwise through 7.89° with respect to the corresponding lines for the austenite. If $\kappa = -1$ the sense of rotation is reversed.

4. Calculations for macrotwins (ii)

Although two martensitic plates cannot simultaneously be compatible with each other and the austenite at zero energy, they can be compatible with each other across a macrotwin plane if suitably rotated. As in the preceding section we consider the case of two plates with the variants U_1 and U_2 having the same relative volume fraction λ^*. Since the average deformation gradient corresponding to layering U_1 with $U_1 + a \otimes n = RU_2$ in the volume fraction λ^* to $1 - \lambda^*$ is $U_1 + \lambda^* a \otimes n$, we need to solve the equation

$$Q(U_1 + \lambda^* a_2 \otimes n_2) - (U_1 + \lambda^* a_1 \otimes n_1) = d \otimes N,$$

where a_1, n_1 and a_2, n_2 are given by (2.5) with $\kappa = 1$ and $\kappa = -1$ respectively, and where $Q \in SO(3)$ and d, N are to be determined. The solutions are given by

$$Q = \begin{pmatrix} \cos\varphi & -\sin\varphi & 0 \\ \sin\varphi & \cos\varphi & 0 \\ 0 & 0 & 1 \end{pmatrix}$$

with either

$$\varphi = \varphi_1 = 2\tan^{-1}\frac{\rho\eta_3}{(1+\rho)\eta_1}, \qquad N = e_1,$$

or

$$\varphi = \varphi_2 = 2\tan^{-1}\frac{\rho\eta_1}{(1-\rho)\eta_3}, \qquad N = e_2,$$

where

$$\rho = \lambda^* \frac{\eta_3^2 - \eta_1^2}{\eta_1^2 + \eta_3^2}.$$

Thus the possible macrotwin normals are $[100]_{B2}$ and $[010]_{B2}$, as observed. The angle α' between the microtwin planes in each plate is given by

$$\alpha' = 90° + \gamma - \varphi_1 = 92.43° \text{ if } N = e_1,$$
$$\alpha' = 90° - \gamma + \varphi_2 = 85.24° \text{ if } N = e_2.$$

5. Discussion

The observed α angles at distances of more than 500nm from the macrotwin interface are in the ranges 92°-97° for $[100]_{B2}$ macrotwins and 83°-86° for $[010]_{B2}$ macrotwins, corresponding to the predicted values of $\alpha = 93.76°$ and $\alpha = 86.24°$ respectively. As the macrotwin interface is approached the α angle is observed to decrease, with values α' in the 50-500nm region in the ranges 90°-95° for $[100]_{B2}$ macrotwins and 83°-85° for $[010]_{B2}$ macrotwins. The sense of rotation of the microtwin variants is as predicted.

Suppose Plate I has habit plane normal $m_1 = (\frac{1}{2}\chi(\delta+\tau), \frac{1}{2}\chi(\tau-\delta), 1)$, while Plate II has habit plane normal $m_2 = (\frac{1}{2}\bar{\chi}(\delta+\tau), -\frac{1}{2}\bar{\chi}(\tau-\delta), 1)$. Can we say which choices of the signs χ and $\bar{\chi}$ lead to a macrotwin normal $N = e_1$, and which to a macrotwin normal $N = e_2$? This is difficult to answer directly from the TEM observations because the angles calculated in Section 3 do not depend on these signs.

A possible mechanism for the selection of N is that when two austenite-martensite interfaces propagate towards each other, they contact first along the common line of their two habit-planes. Up to this time, the deformation has close to zero energy. The process by which the wedge-shaped regions between the plates close up is unclear, but the formation of the final macrotwin is presumably aided if the common line lies in the macrotwin plane. This is the case for $N = e_1$ if and only if $\chi = -\bar{\chi}$, and for $N = e_2$ if and only if $\chi = \bar{\chi}$. On the other hand, the calculations in Section 4 imply that given Plate I, there are two rotations R_1 and R_2 which make it compatible with Plate II across the macrotwin planes with normals $N = e_1$ and $N = e_2$ res[pectively. These rotations are quite close to one another, the angle of rotation of $R_1 R_2^{-1}$ being $\varphi_1 - \varphi_2 = 2.33°$. The angle of rotation of R_1 is 1.75° if $\chi = \bar{\chi}$, and 7.99° if $\chi = -\bar{\chi}$, while that of R_2 is 1.63° if $\chi = \bar{\chi}$, and 7.99° if $\chi = -\bar{\chi}$. Whether the larger angles of rotation when $\chi = -\bar{\chi}$ make this case less likely is unclear. In one case (see [6]) two plates were observed to make contact across both e_1 and e_2 at either ends of a curved macrotwin interface.

In the less symmetrical situation in which the two plates are composed of the same two variants but with reversed volume fractions, using either the same or different microtwins, it is surprisingly still true that the common line of the two habit planes can lie in a zero-energy macrotwin plane. Research is in progress to understand whether there are features of the microstructure in these cases deducible from the nonlinear elasticity model which might explain either why they are unlikely to arise, or why they are difficult to see in TEM images.

To summarise, the observations are consistent with the hypothesis that the macrotwins indeed arise from coalescence of two plates with differ-

ent habit planes, and that these plates remain relatively undistorted in the transformation process except near the macrotwin interface, where achieving compatibility necessarily introduces stresses.

Our work can be thought of as a small step towards a better understanding of pattern formation due to displacive phase transformations. Of course the generation of microstructure is a dynamic process, which one might hope to treat using appropriate dynamic equations at the continuum level. However it is not clear which dynamic equations in the bulk and for the motion of interfaces should be used, and for no such equations would we currently have much hope of making quantitative or qualitative predictions. Like many calculations using the static theory, our work has more the flavour of a consistency check for a scenario of pattern formation, rather than being a genuine prediction starting from the governing equations.

References

1. J.M. Ball. A version of the fundamental theorem for Young measures. In M. Rascle, D. Serre, and M. Slemrod, editors, *Proceedings of conference on 'Partial differential equations and continuum models of phase transitions'*, pages 3–16. Springer Lecture Notes in Physics. No. 359, 1989.
2. J.M. Ball and R.D. James. Fine phase mixtures as minimizers of energy. *Arch. Rat. Mech. Anal.*, 100:13–52, 1987.
3. J.M. Ball and R.D. James. Proposed experimental tests of a theory of fine microstructure, and the two-well problem. *Phil. Trans. Roy. Soc. London A*, 338:389–450, 1992.
4. K. Bhattacharya. Wedge-like microstructure in martensites. *Acta Metallurgica et Materialia*, 39:2431–2444, 1991.
5. K. Bhattacharya. Comparison of geometrically nonlinear and linear theories of martensitic transformation. *Cont. Mech. Thermodyn.*, 5:205–242, 1993.
6. Ph. Boullay, D. Schryvers, and J.M. Ball. Nano-structures at martensite macrotwin interfaces in bulk and splat-cooled $Ni_{65}Al_{35}$. To appear.
7. Ph. Boullay, D. Schryvers, and R.V. Kohn. Bending martensite needles in Ni-Al using 2D elasticity and HRTEM. Phys. Rev. B, in press.
8. A.G. Khachaturyan. Some questions concerning the theory of phase transformations in solids. *Soviet Physics - Solid State*, 8:2163–2168, 1967.
9. A.G. Khachaturyan. *Theory of Structural Transformations in Solids.* John Wiley, 1983.
10. A.G. Khachaturyan and G.A. Shatalov. Theory of macroscopic periodicity for a phase transition in the solid state. *Soviet Physics JETP*, 29:557–561, 1969.
11. A.L. Roitburd. *Kristallografiya*, page 567 ff., 1967. In Russian.
12. A.L. Roitburd. Martensitic transformation as a typical phase transformation in solids. *Solid State Physics*, 33:317–390, 1978.
13. M.S. Wechsler, D.S. Lieberman, and T.A. Read. On the theory of the formation of martensite. *Trans. AIME J. Metals*, 197:1503–1515, 1953.